Universität des Saarlandes

Fachrichtung 6.1 – Mathematik

Preprint

Diffusion and Regularization of Vector- and Matrix-Valued Images

Joachim Weickert and Thomas Brox

Preprint No. 58
Saarbrücken 2002

Universität des Saarlandes

Fachrichtung 6.1 – Mathematik

Diffusion and Regularization of Vector- and Matrix-Valued Images

Joachim Weickert

Saarland University
Faculty of Mathematics and
Computer Science, Building 27.1
P. O. Box 15 11 50
66041 Saarbrücken
Germany
E-Mail:
weickert@mia.uni-saarland.de

Thomas Brox

Saarland University
Faculty of Mathematics and
Computer Science, Building 27.1
P. O. Box 15 11 50
66041 Saarbrücken
Germany
E-Mail:
brox@mia.uni-saarland.de

submitted: March 31, 2002

Preprint No. 58

Saarbrücken 2002

Edited by
FR 6.1 – Mathematik
Im Stadtwald
D–66041 Saarbrücken
Germany

Fax: + 49 681 302 4443
e-mail: preprint@math.uni-sb.de
WWW: http://www.math.uni-sb.de/

Abstract

The goal of this paper is to present a unified description of diffusion and regularization techniques for vector-valued as well as matrix-valued data fields. In the vector-valued setting, we first review a number of existing methods and classify them into linear and nonlinear as well as isotropic and anisotropic methods. For these approaches we present corresponding regularization methods. This taxonomy is applied to the design of regularization methods for variational motion analysis in image sequences. Our vector-valued framework is then extended to the smoothing of positive semidefinite matrix fields. In this context a novel class of anisotropic diffusion and regularization methods is derived and it is shown that suitable algorithmic realizations preserve the positive semidefiniteness of the matrix field without any additional constraints. As an application, we present an anisotropic nonlinear structure tensor and illustrate its advantages over the linear structure tensor.

AMS Subject Classification: 68T10, 68T45, 35J60, 35K55
Key words: image processing, diffusion filtering, regularization methods

Contents

1 Introduction

In digital image processing, vector- and matrix-valued data sets are becoming increasingly important. This is caused by rapidly dropping prices for color imaging devices as well as by novel imaging techniques such as Diffusion Tensor MRI. Often these data suffer from noise creating the need for image restoration methods that allow to remove the noise without severely affecting important structures such as image discontinuities (edges).
In the present paper we will review some recent techniques that achieve this goal by using nonlinear diffusion or regularization approaches. A unifying description is presented that includes diffusion and regularization techniques, linear and nonlinear approaches as well as isotropic and anisotropic methods for vector- or matrix-valued data sets. However, we will not only confine ourselves to the review of existing techniques, we will also present several novel approaches that have not been considered before. Since this paper is mainly intended as a means to communicate the essential ideas and structural similarities, we do not go very deeply into mathematical details. Such details and full proofs can be found in more specialized publications.
Our paper is organized as follows. In Section 2 we first review diffusion techniques for vector-valued images before we present energy functionals for corresponding regularization methods. This taxonomy is then used for classifying variational approaches for motion analysis in image sequences. Section 3 is devoted to matrix-valued image processing. In analogy to our discussions in the vector-valued case, we present diffusion and regularization methods in the isotropic and anisotropic setting. The latter methods are studied here for the first time. We argue that these methods are capable of preserving the positive semidefiniteness of an initial matrix field without the need to impose additional constraints. Finally we apply our ideas to the generalization of the linear structure tensor, a very successful tool for analysing corners, textures and flow-like structures, to the nonlinear setting. Our paper is concluded with a summary in Section 4.

2 Vector-Valued Filtering

2.1 Diffusion of Vector-Valued Images

Vector-valued images arise for example as color images, multi-spectral satellite images and multi-spin echo MR images. Diffusion filtering of some multichannel image $f = (f_1(x, y), ..., f_m(x, y))^\top$ may be based on one of the following evolutions:

(a) *Homogeneous diffusion* ([14] in the scalar case):

$$\partial_t u_i \;=\; \Delta u_i \qquad (i = 1, ..., m) \tag{1}$$

(b) *Linear isotropic diffusion* ([9] in the scalar case):

$$\partial_t u_i \;=\; \mathrm{div}\left(g\Big(\sum_j |\nabla f_j|^2 \Big)\, \nabla u_i \right) \qquad (i = 1, ..., m) \tag{2}$$

(c) *Linear anisotropic diffusion* ([15] in the scalar case):

$$\partial_t u_i \;=\; \mathrm{div}\left(D\Big(\sum_j \nabla f_j \nabla f_j^\top \Big)\, \nabla u_i \right) \qquad (i = 1, ..., m) \tag{3}$$

(d) *Nonlinear isotropic diffusion [10]:*

$$\partial_t u_i \;=\; \mathrm{div}\left(g\Big(\sum_j |\nabla u_j|^2 \Big)\, \nabla u_i \right) \qquad (i = 1, ..., m) \tag{4}$$

(e) *Nonlinear anisotropic diffusion [33]:*

$$\partial_t u_i \;=\; \mathrm{div}\left(D\Big(\sum_j \nabla u_j \nabla u_j^\top \Big)\, \nabla u_i \right) \qquad (i = 1, ..., m) \tag{5}$$

with f as initial condition:

$$u_i(x, y, 0) = f_i(x, y) \qquad (i = 1, ..., m). \tag{6}$$

Here, g denotes a scalar-valued diffusivity, and D is a positive definite diffusion matrix. The diffusivity $g(s^2)$ is a decreasing function in its argument. Moreover, we assume that the flux function $g(s^2)s$ is nondecreasing in s. One may e.g. use [19]

$$g(s^2) \;=\; \alpha + \frac{1}{\sqrt{\beta^2 + s^2}}. \tag{7}$$

with some small positive numbers α and β. In the linear case this ensures that at edges of the initial image f, where $\sum_j |\nabla f_j|^2$ is large, the diffusivity $g(\sum_j |\nabla f_j|^2)$ is close to zero. Consequently, diffusion at edges is inhibited. In the nonlinear case one introduces a feedback by adapting the diffusivity g

to the evolving image u. In physics, a diffusion process with a scalar-valued diffusivity is called *isotropic*, since its diffusive behavior does not depend on the direction.
Anisotropic diffusion with a direction depending behavior may be realized by replacing the scalar-valued diffusivity g by some positive definite diffusion matrix D. One may design the diffusion matrix D such that diffusion along edges of f or u is preferred and diffusion across edges is inhibited. This may be very useful in cases when noisy edges are present.
How can edge directions in some vector-valued image f be measured? Di Zenzo [7] has proposed to consider the matrix $\sum_j \nabla f_j \nabla f_j^\top$. It serves as a structure tensor for vector-valued images since its eigenvectors v_1, v_2 describe the directions of highest and lowest contrast. This contrast is given by the corresponding eigenvalues μ_1 and μ_2.
A natural choice for the design of some diffusion matrix D as a function of a vector-valued image f would thus be to specify its eigenvectors as the eigenvectors v_1, v_2 of $\sum_j \nabla f_j \nabla f_j^\top$, and its eigenvalues λ_1, λ_2 via

$$\lambda_1 = g(\mu_1), \tag{8}$$
$$\lambda_2 = g(\mu_2), \tag{9}$$

with a diffusivity function g as e.g. in (7).

Remark 1. The fact that in the preceding models the same diffusivity or diffusion matrix is used for all channels ensures that the evolutions between the channels are synchronized. This prevents e.g. that discontinuities are created at different locations in each channel.

Remark 2. Let $J \in \mathbb{R}^{2\times 2}$ be symmetric with eigenvectors v_1, v_2 and eigenvalues μ_1, μ_2:

$$J = \mu_1 v_1 v_1^\top + \mu_2 v_2 v_2^\top. \tag{10}$$

A formal way to extend some scalar-valued function $g(s^2)$ to a matrix-valued function $g(J)$ is to define

$$g(J) := g(\mu_1) v_1 v_1^\top + g(\mu_2) v_2 v_2^\top. \tag{11}$$

With this notation we may characterize the linear and nonlinear isotropic models by their diffusivities $g(\sum_j \nabla f_j^\top \nabla f_j)$ and $g(\sum_j \nabla u_j^\top \nabla u_j)$, while their anisotropic counterparts are given by $g(\sum_j \nabla f_j \nabla f_j^\top)$ and $g(\sum_j \nabla u_j \nabla u_j^\top)$. Hence, isotropic and anisotropic models only differ by the location of the transposition.

Remark 3. It should be noted that the preceding models are not the only diffusion methods that have been proposed for processing vector-valued images. For alternative approaches the reader is referred to [3, 17, 26, 30, 35].

Remark 4. The requirement of having a nondecreasing flux $g(s^2)s$ has been introduced in order to ensure well-posedness in the nonlinear setting using classical frameworks such as maximal monotone operators [4]. It is also possible to use more sophisticated models that allow contrast enhancement. In this case one can establish well-posedness results if some Gaussian presmoothing is introduced in the diffusivity or the diffusion matrix [5, 34].

Experiments. Figure 1 illustrates the effect of the different smoothing strategies for a noisy color image with three channels corresponding to the red, green and blue components. We observe that homogeneous diffusion performs well with respect to denoising, but does not respect image edges. Space-variant linear isotropic diffusion, however, may suffer from noise sensitivity as strong noise may be misinterpreted as an important edge structure where the diffusivity is reduced. Anisotropic linear diffusion allows smoothing along edges, but reduces smoothing across them. This leads to a better performance than isotropic linear diffusion if images are noisy. We can also observe that nonlinear models give better results than their linear counterparts. This is not surprising, since the nonlinear models adapt the diffusion process to the evolving image instead of the initial one.

2.2 Regularization Methods for Vector-Valued Images

Let us now explain some connections between the preceding vector-valued diffusion filters and regularization methods for vector-valued data. To this end we consider minimizers of the following energy functionals over some rectangular image domain Ω:

(a) *homogeneous regularization:*

$$E_{HV}(u) \;=\; \frac{1}{2}\int_\Omega \Big(|f-u|^2 + \alpha \sum_k |\nabla u_k|^2\Big)\, dx\, dy \tag{12}$$

(b) *linear isotropic regularization:*

$$E_{LIV}(u) \;=\; \frac{1}{2}\int_\Omega \Big(|f-u|^2 + \alpha\, g\Big(\sum_j |\nabla f_j|^2\Big) \sum_k |\nabla u_k|^2\Big)\, dx\, dy \tag{13}$$

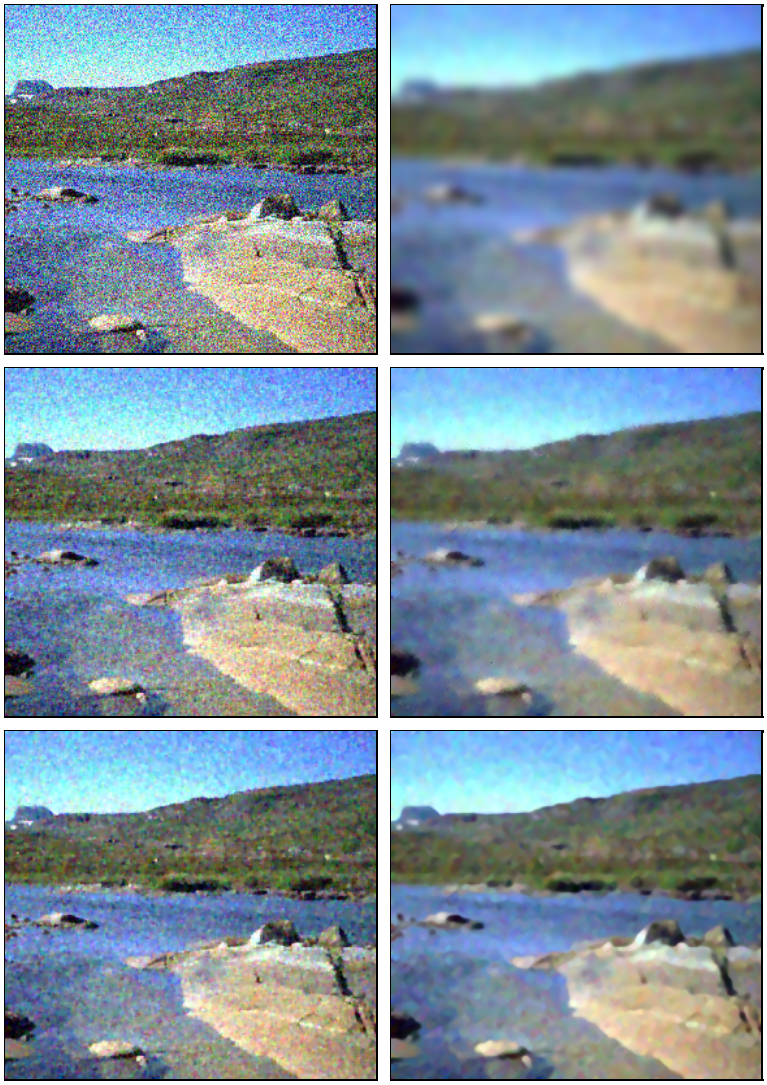

Figure 1: (a) Top Left: Noisy color image. (b) Top Right: Homogeneous diffusion. (c) Middle Left: Linear isotropic diffusion. (d) Middle Right: Linear anisotropic diffusion. (e) Bottom Left: Nonlinear isotropic diffusion. (f) Bottom Right: Nonlinear anisotropic diffusion.

(c) *linear anisotropic regularization:*

$$E_{LAV}(u) \;=\; \frac{1}{2}\int_\Omega \Big(|f-u|^2 + \alpha \sum_k \nabla u_k^\top \, g\Big(\sum_j \nabla f_j \nabla f_j^\top\Big)\, \nabla u_k\Big)\, dx\, dy \tag{14}$$

(d) *nonlinear isotropic regularization:*

$$E_{NIV}(u) \;=\; \frac{1}{2}\int_\Omega \Big(|f-u|^2 + \alpha\, \Psi\Big(\sum_k |\nabla u_k|^2\Big)\Big)\, dx\, dy \tag{15}$$

(e) *nonlinear anisotropic regularization:*

$$E_{NAV}(u) \;=\; \frac{1}{2}\int_\Omega \Big(|f-u|^2 + \alpha\, \mathrm{tr}\, \Psi\Big(\sum_k \nabla u_k \nabla u_k^\top\Big)\Big)\, dx\, dy \tag{16}$$

with some penalizing function $\Psi(s^2)$ that is differentiable in its argument and convex in s. Moreover, we assume that there exist constants $c_1, c_2 > 0$ such that $c_1 s^2 \le \Psi(s^2) \le c_2 s^2$ for all s. In the experiments for this paper we use the Nashed–Scherzer regularizer [19]

$$\Psi(s^2) \;:=\; \alpha s^2 + \sqrt{\beta^2 + s^2} \tag{17}$$

with some small parameters $\alpha, \beta > 0$. Its derivative is given by the diffusivity (7). Under the preceding assumptions one can show that the convex minimization problems (12)–(16) are well-posed in the Sobolev space $H^1(\Omega) \times ... \times H^1(\Omega)$. Their unique solution satisfies the following Euler-Lagrange equations:

(a) *homogeneous regularization:*

$$\frac{u_i - f_i}{\alpha} \;=\; \Delta u_i \qquad (i = 1, ..., m) \tag{18}$$

(b) *isotropic linear regularization:*

$$\frac{u_i - f_i}{\alpha} \;=\; \mathrm{div}\, \Big(g\Big(\sum_k |\nabla f_k|^2\Big)\, \nabla u_i\Big) \qquad (i = 1, ..., m) \tag{19}$$

(c) *anisotropic linear regularization:*

$$\frac{u_i - f_i}{\alpha} \;=\; \mathrm{div}\, \Big(g\Big(\sum_k \nabla f_k \nabla f_k^\top\Big)\, \nabla u_i\Big) \qquad (i = 1, ..., m) \tag{20}$$

(d) *isotropic nonlinear regularization:*

$$\frac{u_i - f_i}{\alpha} = \operatorname{div}\Big(\Psi'\Big(\sum_k |\nabla u_k|^2\Big)\,\nabla u_i\Big) \qquad (i = 1, ..., m) \qquad (21)$$

(e) *anisotropic nonlinear regularization:*

$$\frac{u_i - f_i}{\alpha} = \operatorname{div}\Big(\Psi'\Big(\sum_k \nabla u_k \nabla u_k^\top\Big)\,\nabla u_i\Big) \qquad (i = 1, ..., m) \qquad (22)$$

with homogeneous Neumann boundary conditions.
While this is very easy to verify for the cases (a)–(d), the proof for the case (e) is more involved. More details can be found in a recent paper [36] where these anisotropic nonlinear regularizers have been analyzed first.
We may regard the elliptic equations (18)–(22) as fully implicit time discretizations of the parabolic diffusion filters (1)–(4) with initial value f and time step size α. This connection has been used in [27, 24] to establish a scale-space theory for noniterated and iterated scalar-valued regularization methods. The results include well-posedness, maximum-minimum principles, a large family of Lyapunov functionals and convergence to a flat image as $\alpha \to \infty$. This reasoning can also be extended to the vector-valued case. Experiments in [27, 24] showed that even for large regularization parameters α the regularization methods and their diffusion counterparts are visually fairly similar. This is also the case for the vector-valued setting, so we refrain from showing experimental results, since they can hardly be distinguished from those for diffusion filtering.

2.3 Application: Variational Image Sequence Analysis

Let us now apply the preceding concepts to the analysis of image sequences [36].
One of the main goals of image sequence analysis is the recovery of the so-called *optic flow* field. Optic flow describes the apparent motion of structures in the image plane. It can be used in a large variety of applications ranging from the recovery of motion parameters in robotics to the design of efficient algorithms for second generation video compression.
In the following we consider an image sequence $f(x, y, z)$ where $(x, y) \in \Omega$ denotes the location and $z \in [0, Z]$ is the time. We are looking for the optic flow field $\begin{pmatrix} u_1(x,y,z) \\ u_2(x,y,z) \end{pmatrix}$ which describes the correspondence of image structures at different times.

Very frequently it is assumed that image structures do not change their grey value over time. Therefore, along their path $(x(z), y(z))$ one obtains

$$0 \;=\; \frac{df(x(z),\, y(z),\, z)}{dz} \;=\; f_x u_1 + f_y u_2 + f_z. \tag{23}$$

This brightness constancy assumption is called *optic flow constraint (OFC)*. It is not sufficient to determine $u := (u_1, u_2)$ uniquely. As a remedy, a regularizing smoothness constraint may be introduced such that the optic flow problem can be solved within a variational framework. We may recover the optic flow as minimizer of some convex functional of type

$$E(u) := \int_\Omega \Big(\tfrac{1}{2} \underbrace{(f_x u_1 + f_y u_2 + f_z)^2}_{\text{data term}} + \alpha \underbrace{V(\nabla f, \nabla u)}_{\text{regularizer}} \Big)\, dx\, dy \tag{24}$$

where $V(\nabla f, \nabla u)$ penalizes deviations from (piecewise) smoothness, and $\nabla u := (\nabla u_1, \nabla u_2)$. The corresponding gradient descent equations are given by

$$\partial_t u_1 \;=\; \partial_x V_{u_{1x}} + \partial_y V_{u_{1y}} \;-\; \tfrac{1}{\alpha} f_x \Big(f_x u_1 + f_y u_2 + f_z \Big), \tag{25}$$

$$\partial_t u_2 \;=\; \partial_x V_{u_{2x}} + \partial_y V_{u_{2y}} \;-\; \tfrac{1}{\alpha} f_y \Big(f_x u_1 + f_y u_2 + f_z \Big). \tag{26}$$

This diffusion–reaction system allows to recover the optic flow u as solution for $t \to \infty$. We observe that the regularizer $V(\nabla f, \nabla u)$ creates the vector-valued diffusion processes

$$\partial_t u_i \;=\; \partial_x V_{u_{ix}} + \partial_y V_{u_{iy}} \qquad (i = 1, 2). \tag{27}$$

Specific choices of V allow to design regularizers that smooth the flow field, but respect semantically important image discontinuities or flow discontinuities. In the first case, we call the method *image-driven*, in the second case it is a *flow-driven* method. If the regularizer corresponds to an isotropic diffusion process, it is named *isotropic*, otherwise it is an *anisotropic* regularizer. Table 1 gives an overview of the different vector-valued diffusion processes that we have just discussed, and their corresponding optic flow regularizers. Firstly we observe that diffusion filters have been discovered several years ahead of their corresponding optic flow regularizers. Secondly, it becomes clear that image-driven regularizers always correspond to linear diffusion processes, while flow-driven ones can be related to nonlinear diffusion filters.
It is possible to treat all these optic flow methods within a unifying theoretical framework. In [36] the following well-posedness results have been established.

Table 1: Vector-valued diffusion processes and their corresponding optic flow regularizers. In the diffusion context, f denotes the vector-valued initial image and u its evolution. In the optic flow setting, f is the scalar-valued image sequence and u describes the optic flow field.

vector-valued diffusion process $\partial_t u_i = \partial_x V_{u_{ix}} + \partial_y V_{u_{iy}}$	optic flow regularizer $V(\nabla f, \nabla u)$
homogeneous $\partial_t u_i = \Delta u_i$ (scalar case: Iijima 1959 [14])	homogeneous $\sum_{i=1}^{2} \lvert\nabla u_i\rvert^2$ (Horn/Schunck 1981 [13])
linear isotropic $\partial_t u_i = \operatorname{div}\left(g(\sum_j \lvert\nabla f_j\rvert^2)\, \nabla u_i\right)$ (scalar case: Fritsch 1992 [9])	image-driven, isotropic $g(\lvert\nabla f\rvert^2) \sum_{i=1}^{2} \lvert\nabla u_i\rvert^2$ (Alvarez et al. 1999 [1])
linear anisotropic $\partial_t u_i = \operatorname{div}\left(g(\sum_j \nabla f_j \nabla f_j^\top)\, \nabla u_i\right)$ (scalar case: Iijima 1962 [15])	image-driven, anisotropic $\sum_{i=1}^{2} \nabla u_i^\top D(\nabla f)\, \nabla u_i$ (Nagel 1983 [18])
nonlinear isotropic $\partial_t u_i = \operatorname{div}\left(\Psi'(\sum_j \lvert\nabla u_j\rvert^2)\, \nabla u_i\right)$ (Gerig et al. 1992 [10])	flow-driven, isotropic $\Psi\left(\sum_{i=1}^{2} \lvert\nabla u_i\rvert^2\right)$ (Schnörr 1994 [28])
nonlinear anisotropic $\partial_t u_i = \operatorname{div}\left(\Psi'(\sum_j \nabla u_j \nabla u_j^\top)\, \nabla u_i\right)$ (Weickert 1994 [33])	flow-driven, anisotropic $\operatorname{tr} \Psi\left(\sum_{i=1}^{2} \nabla u_i \nabla u_i^\top\right)$ (Weickert/Schnörr 2001 [36])

Theorem 1 *Let $V(\nabla f, \nabla u)$ be one of the optic flow regularizers from Table 1. Moreover, let us assume that*

- *Ψ is differentiable, and $\Psi(s^2)$ is strictly convex in $s \in \mathbb{R}$*

- *There exist* $c_1, c_2 > 0$ *such that* $c_1 s^2 \leq \Psi(s^2) \leq c_2 s^2$ *for all* s.
- $f \in H^1(\Omega \times (0,T))$
- f_x, f_y *are linearly independent in* $\mathrm{L}^2(\Omega)$, *and* $f_x, f_y \in \mathrm{L}^\infty(\Omega)$.

Then the optic flow functional (24) has a unique minimizer $u(z) \in H^1(\Omega) \times H^1(\Omega)$ *that depends in a continuous way on the image sequence* f.

In order to illustrate the influence of the different regularization methods, we used the marbled block sequence of Otte and Nagel (KOGS/IAKS, University of Karlsruhe, Germany) [20]. These images can be downloaded from the web site `http://i21www.ira.uka.de/image-sequences`. The sequence consists of 31 frames of size 512×512. In our case we only used frame 16 and 17. Figure 2 depicts the results for the optic flow magnitude. For better visibility, we also show a detail of the flow magnitude images in Figure 3.
As expected, one can observe that the homogeneous regularization of Horn and Schunck creates very smooth flow fields. It is, however, unsuited to respect any flow discontinuities.
Isotropic image-driven reduces smoothing at all image edges. This may create an oversegmentation of the flow fields, as can be seen from the flow artifacts resulting from the texture of the marbled floor. This oversegmentation influences in particular the flow magnitude, while the flow direction appears to be more stable.
Anisotropic image-driven regularization permits smoothing along image edges. This leads to a more homogeneous flow field than the one from isotropic image-driven smoothing. Larger structures of the marble texture, however, are still visible in this case as well.
Flow-driven models are performing better here. The marble texture, which corresponds to image discontinuities but not to flow discontinuities, does hardly perturb the flow field. Figure 3 shows that, similar to the image-driven case, anisotropic regularization is less affected by these texture artifacts that isotropic smoothing, although the differences are a bit smaller. This shows that anisotropic flow-driven regularization is an interesting technique for optic flow problems where flow discontinuities are important and highly textured image structures are present.

3 Matrix-Valued Filtering

In this section we extend diffusion and regularization methods to fields of matrix-valued data. After giving a motivation of the practical importance of

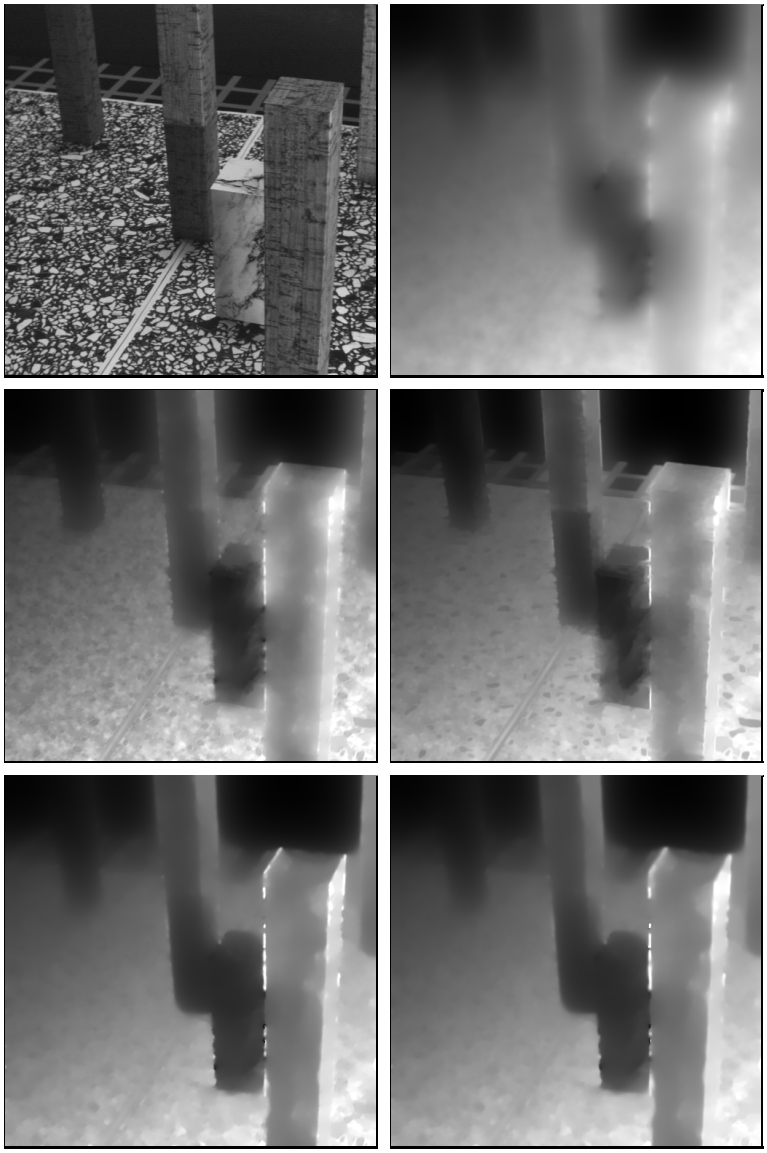

Figure 2: (a) TOP LEFT: Frame 16 of the marbled block sequence (512 × 512 pixels). (b) TOP RIGHT: Optic flow magnitude between Frame 16 and 17 for homogeneous regularization. (c) MIDDLE LEFT: Result for image-driven isotropic regularization (d) MIDDLE RIGHT: Image-driven anisotropic regularization. (e) BOTTOM LEFT: Flow-driven isotropic regularization (f) BOTTOM RIGHT: Flow-driven anisotropic regularization. From [36].

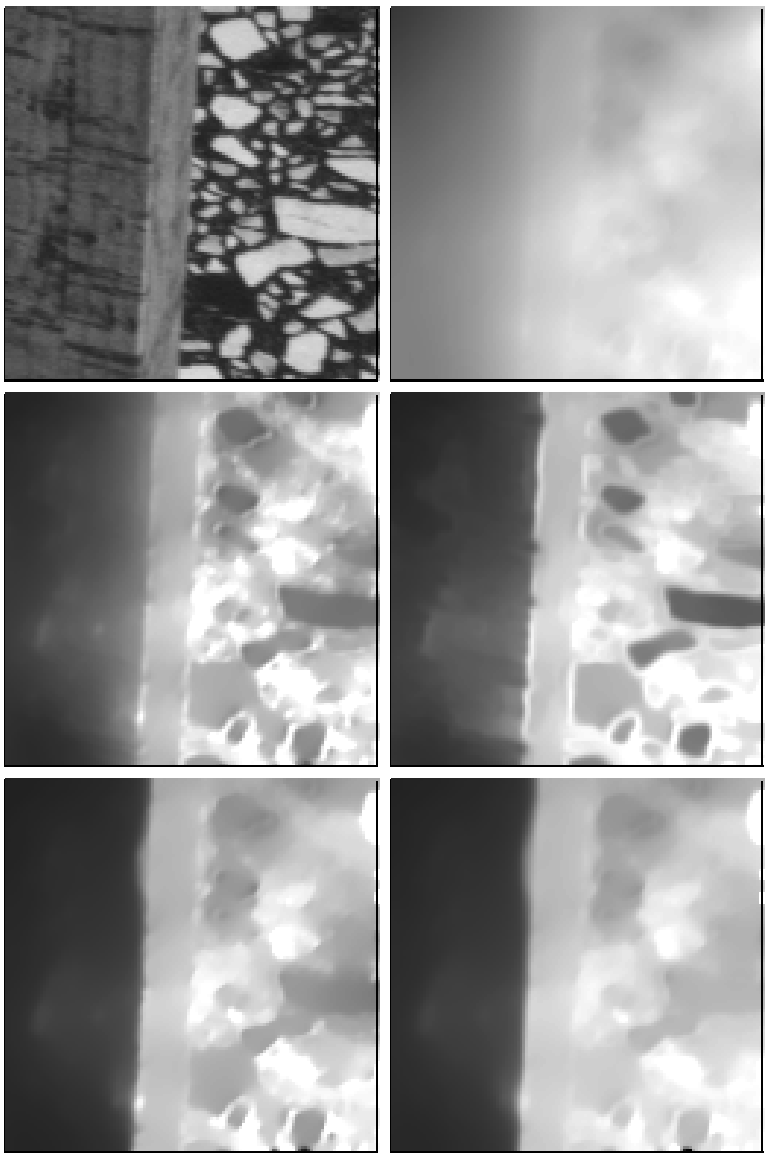

Figure 3: (a) TOP LEFT: Detail from the lower right part of Frame 16 (128×128 pixels). (b) TOP RIGHT: Optic flow magnitude for homogeneous regularization. (c) MIDDLE LEFT: Image-driven isotropic regularization (d) MIDDLE RIGHT: Image-driven anisotropic regularization. (e) BOTTOM LEFT: Flow-driven isotropic regularization (f) BOTTOM RIGHT: Flow-driven anisotropic regularization. For better visibility, the grey values of the optic flow results been transformed by a gamma correction with $\gamma = 0.4$. From [36].

such data sets, we present our models. They also comprise novel anisotropic techniques where a joint diffusion tensor is used instead of a scalar-valued diffusivity. Afterwards we argue that these models are well-suited for the practically important smoothing of positive semidefinite matrix fields, since they maintain the property of positive semidefiniteness without additional projection steps. Finally we study an example where a novel anisotropic nonlinear variant of the structure tensor is constructed and its superiority over linear and nonlinear isotropic structure tensors is illustrated.

3.1 Motivation

The need for smoothing methods for positive semidefinite matrix fields is rapidly growing in the image processing and computer vision community. Let us illustrate this by two examples.

(a) Matrix-valued data fields with positive semidefinite matrices arise for example in all imaging applications where the so-called *structure tensor* is used. The structure tensor of some scalar-valued image v is given by $K_\rho * (\nabla v \nabla v^\top)$ where K_ρ denotes a Gaussian with standard deviation ρ. This Gaussian convolution averages orientation over same scale of order ρ. A principal component analysis of the structure tensor gives information that is highly useful for corner detection [8], texture analysis [25], optic flow computation [2], and even for designing better adaptive numerical algorithms [11, 29].

The structure tensor, however, uses Gaussian convolution of each matrix channel. This is equivalent to linear diffusion filtering with a constant diffusivity. Thus, the question arises whether one can obtain better results by replacing the matrix-valued linear diffusion process by matrix-valued nonlinear diffusion or regularization methods. In this case one would expect to have a better preservation of discontinuities.

(b) Another application consists of *diffusion tensor magnetic resonance imaging (DT-MRI)*, a recent medical image acquisition technique that measures the diffusion characteristics of water molecules in tissues. The resulting diffusion tensor field is a positive semidefinite matrix field that provides valuable information for brain connectivity studies as well as for multiple sclerosis or stroke diagnosis [22].

The search for good smoothing techniques for DT-MRI became a very active research field in the last 3 years. Some authors suggest to perform smoothing of directional images that are used for computing the diffusion tensor field [16, 21, 32]. This comes down to scalar-valued smooth-

ing processes. Other scalar- or vector-valued processes have been applied by smoothing derived expressions such as the eigenvalues and eigenvectors of the diffusion tensor [23, 6, 31] or its fractional anisotropy [21]. Methods that work directly on the diffusion tensor components use linear [37] or nonlinear [12] techniques that filter all channels *independently*, thus performing scalar-valued filtering again. A nonlinear regularization method giving true matrix-valued filtering by coupling the channels via a common diffusivity is due to Tschumperlé and Deriche [31]. They have also included additional projection steps in order to preserve the positive semidefiniteness of the matrix field. Since their diffusivity is scalar-valued, the method may be classified as isotropic. Anisotropic matrix-valued techniques have not been considered so far.

These examples illustrate that there is a clear need for a diffusion and regularization framework for matrix fields. Ideally, it should be compatible with the preceding vector-valued framework and it should take into account matrix-specific requirements such as the preservation of positive semidefiniteness. Below we shall describe such a framework for filtering matrix fields in an isotropic or anisotropic way. Since the linear isotropic and anisotropic cases are less important in practice, we focus on nonlinear methods. The linear strategies can be extended from the vector-valued situation in the same way as is described in the nonlinear setting.

3.2 Matrix-Valued Filter Design

Let us consider some matrix field $F(x) = (f_{kl}(x))$. A regularized version $U(x,\alpha) = (u_{kl}(x,\alpha))$ can be obtained by minimizing

$$E_{IM}(U) \;=\; \frac{1}{2}\int_\Omega \Big(\|F-U\|^2 + \alpha\,\Psi\Big(\mathrm{tr}\sum_{k,l}\nabla u_{kl}\nabla u_{kl}^\top\Big)\Big)\,dx\,dy \tag{28}$$

in the isotropic case, and

$$E_{AM}(U) \;=\; \frac{1}{2}\int_\Omega \Big(\|F-U\|^2 + \alpha\,\mathrm{tr}\,\Psi\Big(\sum_{k,l}\nabla u_{kl}\nabla u_{kl}^\top\Big)\Big)\,dx\,dy \tag{29}$$

in the anisotropic case. We assume that the penalizer Ψ satisfies the same conditions that we imposed in the vector-valued context. As matrix norm, we use the rotationally invariant Frobenius norm

$$\|F\| := \Big(\sum_{k,l} f_{kl}^2\Big)^{1/2}. \tag{30}$$

It guarantees that both energy functionals are rotationally invariant.
Note the large structural similarities between the isotropic and the anisotropic functional: only the order of the penalizer and the trace operator is exchanged. One may also write the isotropic regularizer in a slightly simpler form as $\Psi(\sum_{k,l} |\nabla u_{k,l}|^2)$.
The Euler–Lagrange equations to the isotropic functional (28) and its anisotropic counterpart (29) are given by

$$\frac{u_{ij} - f_{ij}}{\alpha} = \operatorname{div}\Big(\Psi'\Big(\sum_{k,l} \nabla u_{kl}^\top \nabla u_{kl}\Big)\, \nabla u_{ij}\Big) \qquad \forall\, i,j, \tag{31}$$

$$\frac{u_{ij} - f_{ij}}{\alpha} = \operatorname{div}\Big(\Psi'\Big(\sum_{k,l} \nabla u_{kl} \nabla u_{kl}^\top\Big)\, \nabla u_{ij}\Big) \qquad \forall\, i,j. \tag{32}$$

These systems of elliptic PDEs may be regarded as implicit time discretizations of the isotropic resp. anisotropic matrix-valued diffusion processes

$$\partial_t u_{ij} = \operatorname{div}\Big(\Psi'\Big(\sum_{k,l} \nabla u_{kl}^\top \nabla u_{kl}\Big)\, \nabla u_{ij}\Big) \qquad \forall\, i,j, \tag{33}$$

$$\partial_t u_{ij} = \operatorname{div}\Big(\Psi'\Big(\sum_{k,l} \nabla u_{kl} \nabla u_{kl}^\top\Big)\, \nabla u_{ij}\Big) \qquad \forall\, i,j \tag{34}$$

with initial condition

$$u_{ij}(x,0) = f_{ij}(x) \qquad \forall\, i,j \tag{35}$$

and time step size α. The isotropic diffusivity may be simplified to the expression $\Psi'(\sum_{k,l} |\nabla u_{kl}|^2)$.
As in the vector-valued case, one may also use diffusivities $\Psi'(s^2)$ with nonmonotone flux functions $\Psi'(s^2)s$, if in their argument u_{kl} is replaced by a Gaussian-smoothed variant $K_\sigma * u_{kl}$.
While the preceding isotropic regularization or diffusion methods are also part of the models of Tschumperlé and Deriche [31], their anisotropic counterparts are studied for the first time in the present paper. In Subsection 3.4 we shall see that anisotropy may lead to significantly improved results.
Our initial motivation for considering matrix-valued smoothing processes stems from the quadratic case with symmetric matrices that are positive semidefinite. However, it should be noted that our matrix-valued models are not restricted to quadratic matrices: They may be applied to the smoothing of arbitrary $n \times m$ matrix fields. In particular, we may regard an n-dimensional vector as an $n \times 1$ matrix. In this case it follows directly that the matrix-valued diffusion and regularization models comprise our vector-valued ones that we discussed before.

Another point that is worth mentioning is that the preceding matrix-valued smoothing processes use diffusivities or diffusion tensors that are identical for all matrix channels. As in the vector-valued case this ensures that the filtering behavior at edges remains synchronized. Moreover, it has an additional interesting consequence that shall be discussed next.

3.3 Preservation of Positive Semidefiniteness

Let us go back to quadratic matrix fields that are positive semidefinite. In this case a natural requirement for a practically useful smoothing method is that it should not destroy the positive semidefiniteness of the initial matrix field. By construction of our continuous filters it is obvious that symmetric matrix fields remain symmetric under filtering. In order to understand why the nonnegativity of the eigenvalues is preserved as well, it is helpful to consider a finite difference setting.

The sketch of the proof for the discrete diffusion case is as follows. With a slight abuse of notation, let f_{ij} be a discretization of the (i,j) component of the vector field $F(x)$. We may regard f_{ij} as a vector whose components describe the grey values of the (i,j) component at all pixel locations. Let us consider some suitably small time step size τ and let $u^k = (u_{ij})^k$ represent in a similar way some discretization of the matrix field $U(x,t)$ at time level $t = k\tau$. In [34] it is shown that there exist finite difference schemes for diffusion filtering such that $u_{i,j}^{k+1}$ may be obtained from $u_{i,j}^k$ by a matrix–vector multiplication:

$$u_{ij}^0 = f_{ij} \qquad \forall\, i,j \tag{36}$$

$$u_{ij}^{k+1} = A(u_{1,1}^k, ..., u_{n,n}^k)\; u_{ij}^k \qquad \forall\, i,j, \quad \forall\, k \geq 0 \tag{37}$$

where the matrix A has unit row sums and all entries are nonnegative. Since we have a common diffusivity or diffusion tensor for all channels, it follows that A is identical for all channels:

$$A = A(u_{1,1}^k, ..., u_{n,n}^k). \tag{38}$$

Thus, the discrete iteration scheme performs convex combinations of the matrices from the iteration level k in order to obtain the result at level $k+1$. Since convex combinations of positive semidefinite matrices are positive semidefinite again (see e.g. the proof of Proposition 2 in [36]), it follows that the positive semidefiniteness of the initial matrix field is preserved for all iteration levels.

It should be noted that this reasoning depends strongly on the use of a joint diffusivity or diffusion tensor for all matrix channels. Thus, models that apply

different diffusivities in each channel may not preserve positive semidefinite matrix fields unless additional projection steps are introduced (cf. [31]).

3.4 Example: Nonlinear Structure Tensors

Let us now illustrate the usefulness of nonlinear smoothing strategies for matrix-valued data sets by investigating nonlinear versions of the structure tensor that we mentioned in Subsection 3.1.
Given some image v, we consider the tensor product

$$F := (f_{ij}) := \nabla v \nabla v^\top \tag{39}$$

The linear structure tensor computes the convolution $K_\rho * (\nabla v \nabla v^\top)$, where K_ρ denotes a Gaussian with standard deviation ρ. This is equivalent to the linear matrix valued diffusion process

$$\partial_t u_{ij} = \Delta u_{ij} \qquad \forall\, i,j \tag{40}$$

$$u_{ij}(x,0) = f_{ij}(x) \qquad \forall\, i,j \tag{41}$$

with stopping time $T = \frac{1}{2}\,\rho^2$.
Figure 4(a) shows a synthetic test image where we have two regions with homogeneous orientation transitions. These two regions are separated by an orientation discontinuity. An ideal orientation measure would average the orientation information within each region without affecting the orientation discontinuity.
In Figure 4(b) we can see all four components of the structure tensor field when the preceding linear diffusion process is applied. This process blurs each of the tensor components. While this is desirable within the same region, it also blurs the matrix components at orientation discontinuities. If one wants to avoid this shortcoming, one has to use adaptive filters.
A first attempt along these lines is shown in Figure 4(c). It depicts the structure tensor field when the linear diffusion process (40) has been replaced by the isotropic nonlinear evolution (33) with a diffusivity of type (7). We observe that this process does respect orientation discontinuities. On the other hand, it may even be too conservative: at discontinuities, diffusion is stopped in all directions. This may lead to problems in noisy or textured images, where spatial smoothing of the tensor components does not take place.
Anisotropic matrix-valued diffusion filtering on the basis of equations (34) and (7) is illustrated in Figure 4(d). At discontinuities, only diffusion across the discontinuity is inhibited, while diffusion along the discontinuity is still maintained. As one would expect, this leads to the desired matrix averaging

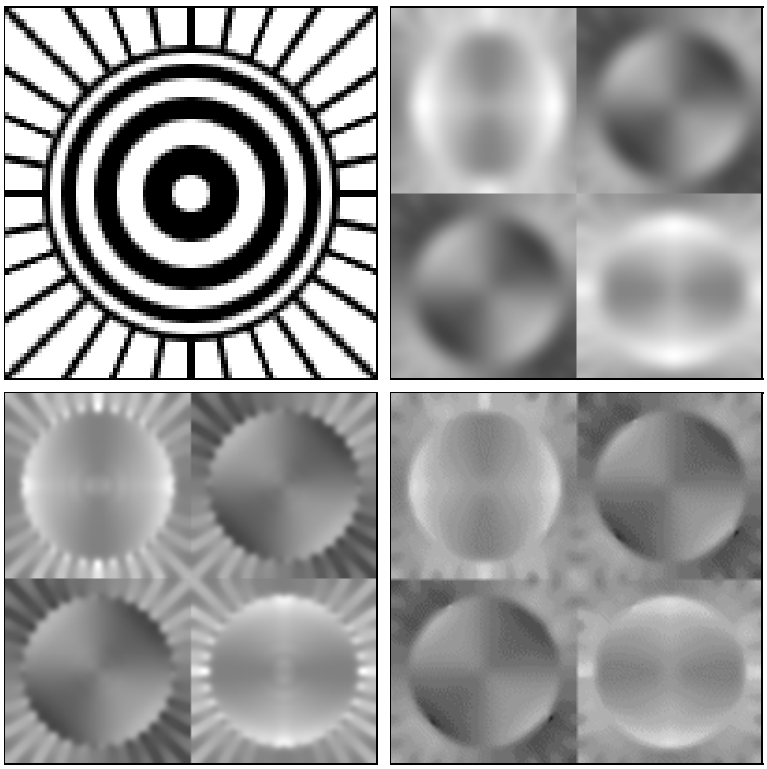

Figure 4: (a) Top Left: Synthetic test image. (b) Top Right: Structure tensor components with matrix-valued linear diffusion filtering. (c) Bottom Left: Ditto with isotropic nonlinear diffusion filtering. (d) Bottom Right: Ditto with anisotropic nonlinear diffusion filtering.

without blurring across orientation discontinuities. This makes the nonlinear anisotropic structure tensor an interesting candidate for a number of applications where the linear structure tensor has limited performance. We are currently trying to identify such situations in order to quantify the benefits of nonlinear anisotropic structure tensors.

4 Summary

In this paper we have given a unified description of diffusion and regularization methods for vector- and matrix-valued data sets. These ideas have been illustrated by applying them to variational motion analysis and by deriving novel nonlinear structure tensors. Since motion analysis in image sequences is only one representative of a large class of correspondence problems in com-

puter vision, and since the structure tensor is present in a large number of different applications, we are optimistic that this framework is applicable to many more areas than those described here. In our future work we plan to present a detailed theoretical analysis of our models, to carry out research on highly efficient numerical algorithms for these approaches, and to investigate further application areas.

Acknowledgements

Our research on matrix-valued smoothing methods is partly funded by the projects WE 2602/1-1 and SO 363/9-1 of the *Deutsche Forschungsgemeinschaft (DFG)*. This is gratefully acknowledged.

References

[1] L. Alvarez, J. Esclarín, M. Lefébure, and J. Sánchez, *A PDE model for computing the optical flow*, in Proc. XVI Congreso de Ecuaciones Diferenciales y Aplicaciones, Las Palmas de Gran Canaria, Spain, Sept. 1999, pp. 1349–1356.

[2] J. Bigün, G. H. Granlund, and J. Wiklund, *Multidimensional orientation estimation with applications to texture analysis and optical flow*, IEEE Transactions on Pattern Analysis and Machine Intelligence, 13 (1991), pp. 775–790.

[3] P. Blomgren and T. F. Chan, *Color TV: total variation methods for restoration of vector valued images*, IEEE Transactions on Image Processing, 7 (1998), pp. 304–309.

[4] H. Brezis, *Opérateurs maximaux monotones et semi-groupes de contractions dans les espaces de Hilbert*, North Holland, Amsterdam, 1973.

[5] F. Catté, P.-L. Lions, J.-M. Morel, and T. Coll, *Image selective smoothing and edge detection by nonlinear diffusion*, SIAM Journal on Numerical Analysis, 32 (1992), pp. 1895–1909.

[6] O. Coulon, D. C. Alexander, and S. A. Arridge, *A regularization scheme for diffusion tensor magnetic resonance images*, in Information Processing in Medical Imaging – IPMI 2001, M. F. Insana and R. M. Leahy, eds., vol. 2082 of Lecture Notes in Computer Science, Springer, Berlin, 2001, pp. 92–105.

[7] S. Di Zenzo, *A note on the gradient of a multi-image*, Computer Vision, Graphics and Image Processing, 33 (1986), pp. 116–125.

[8] W. Förstner and E. Gülch, *A fast operator for detection and precise location of distinct points, corners and centres of circular features*, in Proc. ISPRS Intercommission Conference on Fast Processing of Photogrammetric Data, Interlaken, Switzerland, June 1987, pp. 281–305.

[9] D. S. Fritsch, *A medial description of greyscale image structure by gradient-limited diffusion*, in Visualization in Biomedical Computing '92, R. A. Robb, ed., vol. 1808 of Proceedings of SPIE, SPIE Press, Bellingham, 1992, pp. 105–117.

[10] G. Gerig, O. Kübler, R. Kikinis, and F. A. Jolesz, *Nonlinear anisotropic filtering of MRI data*, IEEE Transactions on Medical Imaging, 11 (1992), pp. 221–232.

[11] T. Grahs, A. Meister, and T. Sonar, *Image processing for numerical approximations of conservation laws: nonlinear anisotropic artificial dissipation*, Tech. Rep. F8, Institute for Applied Mathematics, University of Hamburg, Germany, Dec. 1998.

[12] K. Hahn, S. Pigarin, and B. Pütz, *Edge preserving regularization and tracking for diffusion tensor imaging*, in Medical Image Computing and Computer-Assisted Intervention – MICCAI 2001, W. J. Niessen and M. A. Viergever, eds., vol. 2208 of Lecture Notes in Computer Science, Springer, Berlin, 2001, pp. 195–203.

[13] B. Horn and B. Schunck, *Determining optical flow*, Artificial Intelligence, 17 (1981), pp. 185–203.

[14] T. Iijima, *Basic theory of pattern observation*, in Papers of Technical Group on Automata and Automatic Control, IECE, Japan, Dec. 1959. In Japanese.

[15] ——, *Observation theory of two-dimensional visual patterns*, in Papers of Technical Group on Automata and Automatic Control, IECE, Japan, Oct. 1962. In Japanese.

[16] S. Keeling, R. Bammer, F. Fazekas, and R. Stollberger, *Total variation denoising for improved diffusion tensor calculation*, in Proc. Eighth Scientific Meeting and Exhibition of the International Society for Magnetic Resonance in Medicine, vol. 8, Denver, CO, Apr. 2000, p. 783.

[17] R. Kimmel, R. Malladi, and N. Sochen, *Images as embedded maps and minimal surfaces: movies, color, texture, and volumetric medical images*, International Journal of Computer Vision, 39 (2000), pp. 111–129.

[18] H.-H. Nagel, *Constraints for the estimation of displacement vector fields from image sequences*, in Proc. Eighth International Joint Conference on Artificial Intelligence, vol. 2, Karlsruhe, West Germany, August 1983, pp. 945–951.

[19] M. Z. Nashed and O. Scherzer, *Least squares and bounded variation regularization with nondifferentiable functionals*, Numerical Functional Analysis and Optimization, 19 (1998), pp. 873–901.

[20] M. Otte and H.-H. Nagel, *Estimation of optical flow based on higher-order spatiotemporal derivatives in interlaced and non-interlaced image sequences*, Artificial Intelligence, 78 (1995), pp. 5–43.

[21] G. J. M. Parker, J. A. Schnabel, M. R. Symms, D. J. Werring, and G. J. Barker, *Nonlinear smoothing for reduction of systematic and random errors in diffusion tensor imaging*, Journal of Magnetic Resonance Imaging, 11 (2000), pp. 702–710.

[22] C. Pierpaoli, P. Jezzard, P. J. Basser, A. Barnett, and G. Di Chiro, *Diffusion tensor MR imaging of the human brain*, Radiology, 201 (1996), pp. 637–648.

[23] C. Poupon, J. Mangin, V. Frouin, J. Régis, F. Poupon, M. Pachot-Clouard, D. Le Bihan, and I. Bloch, *Regularization of MR diffusion tensor maps for tracking brain white matter bundles*, in Medical Image Computing and Computer-Assisted Intervention – MICCAI 1998, W. M. Wells, A. Colchester, and S. Delp, eds., vol. 1496 of Lecture Notes in Computer Science, Springer, Berlin, 1998, pp. 489–498.

[24] E. Radmoser, O. Scherzer, and J. Weickert, *Scale-space properties of nonstationary iterative regularization methods*, Journal of Visual Communication and Image Representation, 11 (2000), pp. 96–114.

[25] A. R. Rao and B. G. Schunck, *Computing oriented texture fields*, CVGIP: Graphical Models and Image Processing, 53 (1991), pp. 157–185.

[26] G. Sapiro, *Geometric Partial Differential Equations and Image Analysis*, Cambridge University Press, Cambridge, UK, 2001.

[27] O. Scherzer and J. Weickert, *Relations between regularization and diffusion filtering*, Journal of Mathematical Imaging and Vision, 12 (2000), pp. 43–63.

[28] C. Schnörr, *Segmentation of visual motion by minimizing convex non-quadratic functionals*, in Proc. Twelfth International Conference on Pattern Recognition, vol. A, Jerusalem, Israel, Oct. 1994, IEEE Computer Society Press, pp. 661–663.

[29] I. Thomas, *Anisotropic adaptation and structure detection*, Tech. Rep. F11, Institute for Applied Mathematics, University of Hamburg, Germany, Aug. 1999.

[30] D. Tschumperlé and R. Deriche, *Constrained and unconstrained PDE's for vector image restoration*, in Proc. Twelfth Scandinavian Conference on Image Analysis, Bergen, Norway, June 2001.

[31] ——, *Diffusion tensor regularization with contraints preservation*, in Proc. 2001 IEEE Computer Society Conference on Computer Vision and Pattern Recognition, vol. 1, Kauai, HI, Dec. 2001, IEEE Computer Society Press, pp. 948–953.

[32] B. Vemuri, Y. Chen, M. Rao, T. McGraw, Z. Wang, and T. Mareci, *Fiber tract mapping from diffusion tensor MRI*, in Proc. First IEEE Workshop on Variational and Level Set Methods in Computer Vision, Vancouver, Canada, July 2001, IEEE Computer Society Press, pp. 73–80.

[33] J. Weickert, *Scale-space properties of nonlinear diffusion filtering with a diffusion tensor*, Tech. Rep. 110, Laboratory of Technomathematics, University of Kaiserslautern, Germany, Oct. 1994.

[34] ——, *Anisotropic Diffusion in Image Processing*, Teubner, Stuttgart, 1998.

[35] ——, *Coherence-enhancing diffusion of colour images*, Image and Vision Computing, 17 (1999), pp. 199–210.

[36] J. Weickert and C. Schnörr, *A theoretical framework for convex regularizers in PDE-based computation of image motion*, International Journal of Computer Vision, 45 (2001), pp. 245–264.

[37] C. Westin, S. E. Maier, B. Khidhir, P. Everett, F. A. Jolesz, and R. Kikinis, *Image processing for diffusion tensor magnetic resonance imaging*, in Medical Image Computing and Computer-Assisted Intervention – MICCAI 1999, C. Taylor and A. Colchester, eds., vol. 1679 of Lecture Notes in Computer Science, Springer, Berlin, 1999, pp. 441–452.